BIOCHEMISTRY
including biophysical chemistry & molecular biology

Article

pubs.acs.org/biochemistry

Olefin Isomerization Regiochemistries during Tandem Action of BacA and BacB on Prephenate in Bacilysin Biosynthesis

Jared B. Parker and Christopher T. Walsh*

Department of Biological Chemistry and Molecular Pharmacology, Harvard Medical School, 240 Longwood Ave, Boston, Massachusetts 02115, United States

Supporting Information

ABSTRACT: BacA and BacB, the first two enzymes of the bacilysin pathway, convert prephenate to an exocylic regioisomer of dihydrohydroxyphenylpyruvate (*ex*-H_2HPP) on the way to the epoxycyclohexanone warhead in the dipeptide antibiotic, bacilysin. BacA decarboxylates prephenate without aromatization, converting the 1,4-diene in prephenate to the endocyclic 1,3-diene in Δ^4,Δ^8-dihydrohydroxyphenylpyruvate (*en*-H_2HPP). BacB then performs an allylic isomerization to bring the diene into conjugation with the 2-ketone in the product Δ^3,Δ^5-dihydrohydroxyphenylpyruvate (*ex*-H_2HPP). To prove that BacA acts regiospecifically on one of the two prochiral olefins in prephenate, we generated 1,5,8-[^{13}C]-chorismate from bacterial fermentation of 5-[^{13}C]-glucose and in turn produced 2,4,6-[^{13}C]-prephenate via chorismate mutase. Tandem action of BacA and BacB gave 2,4,8-[^{13}C]-7*R*-*ex*-H_2HPP, showing that BacA isomerizes only the pro-*R* double bond in prephenate. Nonenzymatic isomerization of the BacA product into conjugation gives only the Δ^3 *E*-geometric isomer of Δ^3,Δ^5-*ex*-H_2HPP. On the other hand, acceleration of the allylic isomerization by BacB gives a mixture of the *E*- and *Z*-geometric isomers of the 7*R*- product, indicating some rerouting of the flux, likely through dienolate geometric isomers.

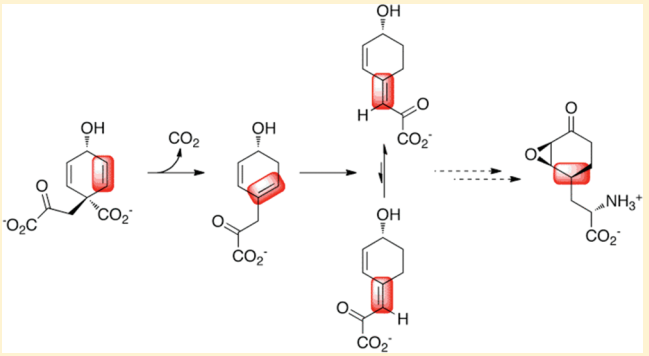

Bacilysin, a dipeptide antibiotic[1−3] produced by *Bacillus subtilis* strains, contains L-Ala and the nonproteinogenic anticapsin, bearing the antibiotic warhead. Anticapsin (Figure 1A) has an expoxycyclohexanone moiety attached to C_3 of alanine. Once taken up by the dipeptide permeases of susceptible bacterial or fungal cells,[4−6] bacilysin is subjected to peptidase action to release the free anticapsin as an analogue of glutamine.[7,8] Anticapsin can then bind to glutaminase domain active sites. The epoxyketone acts as an electrophile to capture the nucleophilic cysteine thiolate in the glutaminase domain of glucosamine-6-phosphate synthetase. Inactivation of both fungal and bacterial glucosamine-6-phosphate synthetases thereby blocks supply of this key amino sugar for cell wall peptidoglycan assembly and leads to the cell lysis that explains the name bacilysin.[8,9]

The epoxycyclohexanone ring in the anticapsin amino acid moiety of bacilysin is an unusual modification. It was presumed to arise by shunting some of the flux from the chorismate pathway[3,10] that would normally yield the aromatic amino acids Phe and Tyr.[11,12] Genetic analysis of bacilysin-producing strains of *B. subtilis* identified a *bac* gene cluster,[13] which was originally identified as five contiguous genes but has since been expanded by biochemical studies to the seven genes *bacA-E* and *ywfGH*. In previous work we have shown that the purified BacAB and YwfGH enzymes can convert prephenate to a 2*S*-tetrahydrotyrosine diastereomer (Figure 1A); there are three stereogenic centers in H_4Tyr, with the C_4 and C_7 stereochemistries previously unassigned.[14] Most notably, the first two enzymes in the pathway, BacA and BacB, act to divert prephenate away from typical aromatization fates to the exocyclic diene Δ^3,Δ^5-dihydrohydroxyphenylpyruvate (*ex*-H_2HPP) (Figure 1A).

The BacA enzyme and homologues we have subsequently characterized in other bacterial pathways to nonproteinogenic dihydro- and tetrahydroamino acid antimetabolites[15,16] catalyze a novel decarboxylative transformation on prephenate. When canonical prephenate decarboxylases liberate CO_2 from prephenate, the electrons that flow into the 1,4-cyclohexadiene ring lead to aromatization as the C_7-OH is ejected and phenylpyruvate is formed.[17,18] By contrast, the BacA subfamily enzymes, during the comparable decarboxylation, capture the electrons by protonation at one end of the starting 1,4-diene (Figure 1B). This leaves the C_7-OH group intact, resulting in formation of a methylene group at C_8 and a net isomerization of the starting 1,4-diene of prephenate into the 1,3 endocyclic diene of the product Δ^4,Δ^8-dihydrohydroxyphenylpyruvate (*en*-H_2HPP). Instead of aromatization of the cyclohexadiene, the ring remains at the dihydroaromatic oxidation state.[14]

BacB acts next and accelerates isomerization to the Δ^3,Δ^5-*ex*-H_2HPP product. The Δ^4 double bond has migrated from being

Received: February 24, 2012
Revised: March 23, 2012
Published: April 6, 2012

ACS Publications © 2012 American Chemical Society

dx.doi.org/10.1021/bi300254u | *Biochemistry* 2012, 51, 3241−3251

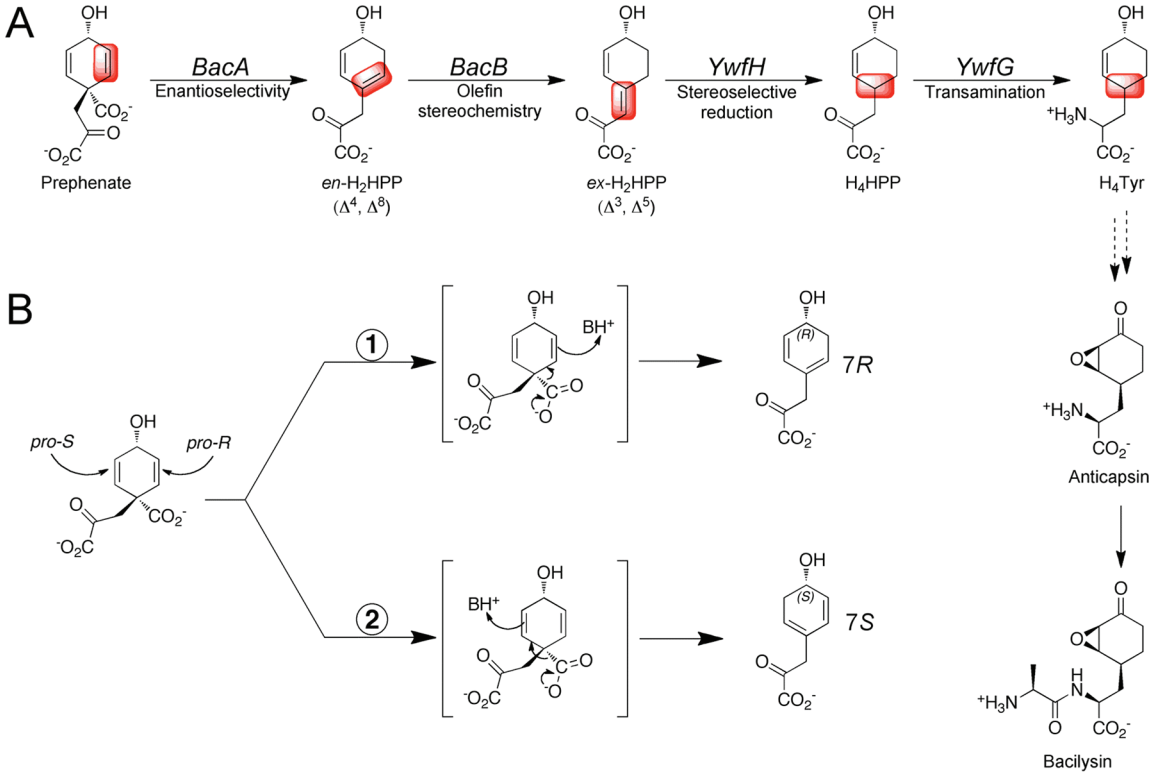

Figure 1. (A) Proposed pathway for the formation of bacilysin from prephenate. Important stereochemical questions are highlighted. (B) Possible enantiomers of *en*-H_2HPP formed from the enzymatic decarboxylation of prephenate by BacA.

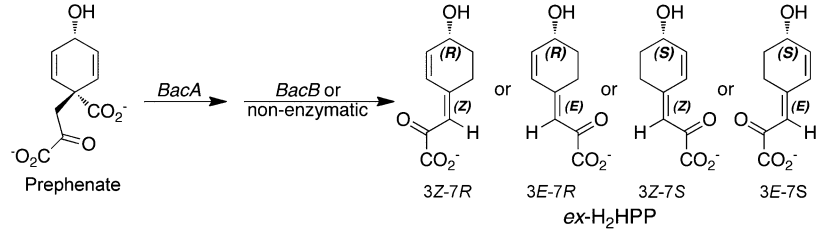

Figure 2. Stereoisomers of *ex*-H_2HPP that could possibly be obtained through the tandem action of BacA decarboxylation of prephenate followed by nonenzymatic or BacB enzymatic isomerization of the internal diene.

endocyclic to the exocyclic Δ^3 position (the other double bond has not moved but the numbering priority has changed (see Figure 1A)). This is a thermodynamically favored allylic isomerization (Δ^4 to Δ^3) bringing the diene into conjugation with the 2-ketone (and generating a yellow chromophore[14]). The rate of isomerization is accelerated about 10^3-fold by BacB.[19] Subsequent conjugate addition of a hydride equivalent from NADH at C_4 by YwfH and transamination by YwfG yields tetrahydrotyrosine, presumably two steps (C_7-alcohol to ketone oxidation and epoxidation of the remaining double bond) away from anticapsin.

To assist in understanding the novel mechanism by which the BacA subfamily separates decarboxylation from aromatization, we have undertaken examination of its stereochemical specificity. The 1,4-diene system in prephenate is symmetric and prochiral, containing pro-*R* and pro-*S* olefins. As shown in path 1 of Figure 1B, decarboxylation and isomerization of the 5,6-olefin (pro-*R*) with protonative quenching at C_6 would yield the 7*R*-OH product (carbon numbering schemes can be viewed in Figure S4 of the Supporting Information). On the other hand, isomerization of the pro-*S* olefin (path 2) would yield the 7*S*-OH product. This stereochemistry may have consequences for the action of subsequent enzymes in the pathway. Analogously, as the allylic isomerization occurs from *en*-H_2HPP to *ex*-H_2HPP, moving the double bond from the endocyclic Δ^4 to the exocyclic Δ^3 position, two possible olefin isomers, the *Z*- or *E*-geometric isomers (Figure 2), could arise for either the 7*R* or 7*S* alcohol generated by BacA action (3*Z*-7*R*, 3*E*-7*R*, 3*Z*-7*S*, and 3*E*-7*S*: Figure 2). In turn, the configuration at those carbon centers could affect recognition and processing by downstream enzymes in this and related pathways which generate distinct chemical outcomes, such as the biosynthesis of the antimetabolite 2,5-dihydrophenylalanine[16] or 2-carboxy-6-hydroxyoctahydroindole (Choi) in aeruginosin assembly.[20]

This paper describes how we have addressed these two stereochemical questions in the bacilysin pathway. With BacA we desired a source of asymmetrically labeled [^{13}C]-prephenate to assess if the BacAB *ex*-H_2HPP product was ^{13}C-enriched at an sp^2 carbon (C_6) (7*S*-alcohol) or sp^3 carbon (C_8) (7*R*-alcohol) (Figure 3). In turn, because of the problematic symmetry of prephenate, we decided to make a labeled [^{13}C]-chorismate as precursor to asymmetric prephenate, convertible via chorismate mutase action. For determination of the *E*-/*Z*-geometric isomer

dx.doi.org/10.1021/bi300254u | *Biochemistry* 2012, 51, 3241−3251

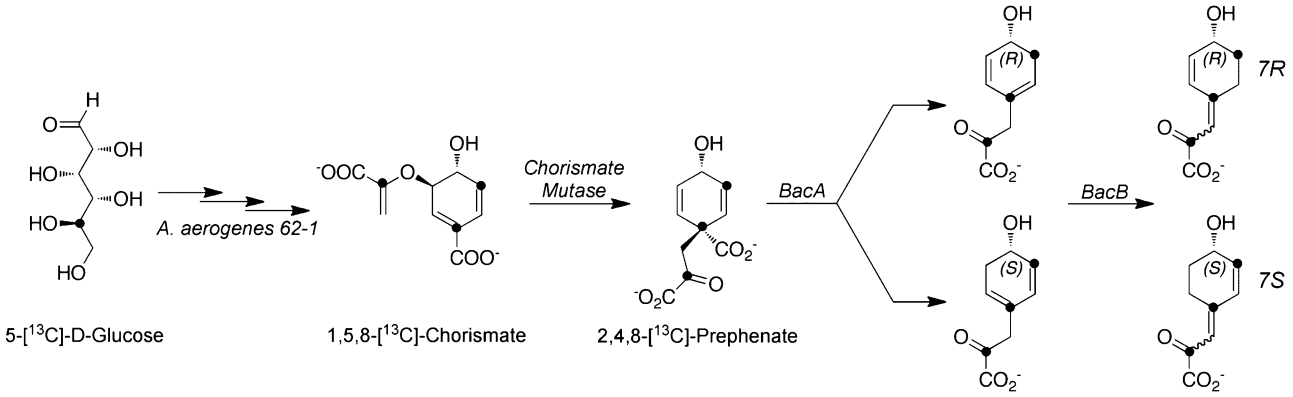

Figure 3. Strategy of positional trace of ^{13}C-label from 5-[^{13}C]-glucose to *ex*-H_2HPP to reveal which *en*-H_2HPP (and thereby *ex*-H_2HPP) enantiomer(s) is being formed via BacA action on prephenate.

content of the *ex*-H_2HPP from BacB action, we were able to separate by HPLC and assign by NMR spectroscopy the two geometric isomers of the Δ^3,Δ^5-exocyclic diene product.

MATERIALS AND METHODS

Materials and Instrumentation. Prephenic acid barium salt and unlabeled chorismic acid were purchased from Sigma-Aldrich. DNA primers were purchased from Integrated DNA Technologies. NMR solvent (D_2O) and [^{13}C]-glucoses were purchased from Cambridge Isotope Laboratories. *B. subtilis* sp. 168 genomic DNA was purchased from ATCC. Herculase II DNA polymerase was purchased from Agilent. Restriction enzymes and T4 DNA ligase were purchased from New England Biolabs. Competent cells were purchased from Invitrogen. Vector (pET-28a) was purchased from Novagen. DNA purification was performed with kits purchased from Qiagen. DNA sequencing was performed by Genewiz. 5 mL His-Trap columns were purchased from GE Healthcare. Any *k*D SDS-PAGE gels were purchased from Bio-Rad. Protein was dialyzed using 10 000 MWCO SnakeSkin Pleated Dialysis tubing from Thermo Scientific, and protein was concentrated using Amicon Ultra 10 000 MWCO centrifugal filters from Millipore. Restriction-grade thrombin was purchased from EMD Biosciences. Hypercarb 5 μm columns were purchased from Thermo Scientific.

^{1}H and 2D NMR spectra were collected on a Varian VNMRS 600 MHz spectrometer equipped with a triple-resonance probe. ^{13}C NMR spectra were recorded on a Varian MR 400 MHz spectrometer (100.497 MHz for ^{13}C) equipped with a OneNMR probe. NMR data were analyzed with ACD/Laboratories software. High-resolution LC/MS data were collected on an Agilent Technologies 6520 Accurate-Mass Q-TOF LC/MS and analyzed with its accompanying software. HPLC was performed on a Beckman Coulter System Gold instrument. Protein purification was performed on an Amersham Pharmacia Biotech AKTA FPLC.

Cloning, Expression, and Purification of Chorismate Mutase and BacAB. The chorismate mutase (CM) gene (*aroH*)[21] was amplified from *B. subtilis* sp. 168 genomic DNA via PCR using primers encoded with *NdeI* and *Bam*HI restriction sites (5′-GGCAGCCATATGATGATTCGCGGAATTC-GCGGAG-3′; 5′-GAATTCGGATCCTTACAATTCAGTAT-TTTTTGTCAATGATAAATCGGGCCTC-3′, respectively). The amplified gene was ligated into vector pET-28a and transformed into chemically competent TOP10 *E. coli* cells (Invitrogen). Proper gene insertion was confirmed by DNA sequencing of the purified plasmid DNA. The sequence-confirmed plasmid was then transformed into chemically competent BL21(DE3) *E. coli* cells for protein expression. The cloning of BacA and BacB and their transformation into BL21(DE3) *E. coli* cells have been previously described.[14] For CM, BacA, and BacB expression, transformed cells were grown at 37 °C in Luria broth media supplemented with 50 μg/mL kanamycin until the $OD_{600\ nm}$ was ∼0.2. The temperature was then reduced to 15 °C for 30 min, and protein expression was induced via addition of 1 mM IPTG. Protein was allowed to express overnight (∼16 h) at 15 °C before cells were harvested by centrifugation (4000*g* for 20 min). Cells/protein were then kept at 4 °C or on ice for all remaining purification steps. Pelleted cells were resuspended in cold lysis buffer (50 mM potassium phosphate pH 8, 500 mM NaCl, 5 mM β-mercaptoethanol, 15 mM imidazole, 5% glycerol) and lysed by two passes of exposure to 5000−15000 psi in an Avestin EmulsiFlex-C5 homogenizer. The cell lysate was clarified via centrifugation (50000*g* for 35 min), and the supernatant was filtered through a 0.45 μm PES syringe filter before being loaded onto a 5 mL His-Trap HP column at 1.5 mL/min via an AKTA FPLC. Bound protein was eluted with a linearly increasing gradient of lysis buffer containing 500 mM imidazole. Fractions were analyzed via SDS-PAGE with visualization by Coomassie blue staining. Proteins were then dialyzed into S-75 buffer (50 mM potassium phosphate pH 8.0, 150 mM NaCl, 1 mM dithiothreitol, and 5% glycerol) using a dialysis membrane. CM aliquots were flash frozen at this point and stored at −80 °C. CM concentration was determined using an extinction coefficient of 8480 M^{-1} cm^{-1} at 280 nm. BacA and BacB were subjected to further purification by gel filtration on a Sephadex 75 26/60 HiLoad column. Fractions were analyzed as described above, and BacA aliquots were flash frozen at this point and stored at −80 °C. BacA concentration was determined using an extinction coefficient of 17 420 M^{-1} cm^{-1} at 280 nm.

The N-terminal hexahistidine tag of BacB was then removed via thrombin treatment at 16 °C. (The His_6-tag was removed to prevent any interactions between the hexahistidine tag and the bound divalent metals of BacB.[19]) Thrombin cleavage was monitored via SDS-PAGE with Coomassie blue visualization. After cleavage was complete (∼16 h), BacB was once again subjected to gel filtration chromatography. The fractions were analyzed by SDS-PAGE, and aliquots of BacB were flash frozen and stored at −80 °C. BacB concentration was determined using an extinction coefficient of 24 410 M^{-1} cm^{-1} at 280 nm.

Assignment of ^{1}H and ^{13}C Spectra of Unlabeled Chorismate and Prephenate. Separately, 3 mg of chorismic acid and potassium prephenate (converted from barium

dx.doi.org/10.1021/bi300254u | *Biochemistry* 2012, 51, 3241−3251

prephenate as previously described[14]) were dissolved in 500 μL of 10 mM potassium phosphate buffer pH 8.0 and purified by loading onto a 100 × 10 mm Hypercarb HPLC column equilibrated in 10 mM potassium phosphate buffer, pH 8.0. Compounds were eluted with a linearly increasing gradient of acetonitrile. Chorismate elution was monitored via UV absorbance at 275 nm. Prephenate elution was monitored by LC/MS run in positive ion detection mode with water + 0.1% formic acid as the mobile phase and acetonitrile + 0.1% formic acid as the eluent. HPLC fractions containing the desired compound (total volume of 3 mL) were frozen and lyophilized to dryness. Dried compound and associated potassium phosphate salt were dissolved in 300 μL of D_2O and placed in a 5 mm D_2O matched Shigemi tube for NMR analysis. Spectral assignments were made via analyses of ^1H, ^{13}C, $^1H-^1H$-gCOSY, $^1H-^{13}C$-gHSQC, and $^1H-^{13}C$-gHMBC spectra. Proton spectra were referenced to residual H_2O (4.79 ppm) while ^{13}C spectra were referenced to the methyl carbon of acetonitrile at (1.47 ppm).[22] (Acetonitrile was spiked into the NMR sample at 0.3% v/v after all necessary spectra were acquired, and an additional ^{13}C experiment was performed to obtain the reference so as not to contaminate the original spectra.) Unless otherwise stated, water suppression (via presaturation) was utilized in all proton spectra collected.

Production of [^{13}C]-Chorismate from [^{13}C]-Glucose. *Aerobacter aerogenes* 62-1 (also known as *Klebsiella pneumoniae* 62-1) was obtained from our lab's strain inventory from ~1990[23] (also available from ATCC #25306). This strain (which lacks chorismate mutase activity) and the associated method for the overproduction of chorismate were developed by Gibson and colleagues.[11,24] Medium A (for the growth of *A. aerogenes* 62-1) and medium B (for the production of chorismate) were made exactly as previously described, except glucose was not added to medium B.[24] 500 mL of medium A was inoculated with a single colony of *A. aerogenes* 62-1 in a 2800 mL wide-mouth baffled flask. The culture was shaken at 200 rpm at 30 °C until the $OD_{600\ nm}$ measured 1.0. The cells were pelleted at 3000*g* at 4 °C for 15 min. The supernatant was discarded, and the cell pellet was gently washed with 250 mL of medium B lacking glucose. The cells were again pelleted via centrifugation as described above. The supernatant was once again discarded, and the cell pellet was resuspended in 250 mL of fresh medium B along with 2 g of either 1-[^{13}C]-glucose or 5-[^{13}C]-glucose (99% enrichment) that had been dissolved in 10 mL of medium B and filtered through a 0.22 μm PES syringe filter. The culture was transferred to a 2800 mL wide-mouth baffled flask and incubated at 30 °C for 15 h while shaking at 200 rpm. The cells were pelleted by centrifugation and discarded.

The supernatant containing the excreted chorismate was filtered through a 0.22 μm PES filter and loaded in 50 mL aliquots onto a 100 × 21.2 mm Hypercarb HPLC column equilibrated in 10 mM potassium phosphate buffer, pH 8.0. The bound compound was eluted via a linearly increasing gradient of acetonitrile. UV absorption at 275 nm was monitored to detect chorismate elution. Fractions containing pure chorismate were initially indentified by a UV-absorbance wavelength scan (λ_{max} = 275 nm, data not shown) and then verified by ^1H NMR spectroscopy (Figures S2B and S4A). Fractions were pooled, frozen, lyophilized to dryness, and stored at −80 °C. Chorismate concentrations were determined by UV absorbance ($\varepsilon_{275\ nm}$ = 2630 M^{-1} cm^{-1}).[10] The ^{13}C enrichment of chorismate was determined by integration of ^1H NMR spectra (satellite peaks of ^{13}C-linked protons) and inverse-gated decoupled ^{13}C NMR spectra collected with an interscan delay time of 150 s to allow full relaxation of the quaternary carbons.[25] [^{13}C]-Chorismate samples were prepped for NMR exactly as described above for unlabeled chorismate.

Conversion of [^{13}C]-Chorismate to [^{13}C]-Prephenate and NMR Assignment. 2.1 mg of [^{13}C]-chorismate was incubated with 145 μg of chorismate mutase in 3 mL of 50 mM potassium phosphate buffer pH 8.0 for 15 h at 21 °C. Reaction progress was monitored by the disappearance of the UV absorbance of chorismate. The reaction was quenched via addition of acetonitrile to 30% v/v and vortexing. The quenched reaction was frozen and lyophilized to dryness. Lyophilized components were resuspended in 500 μL of 10 mM potassium phosphate buffer pH 8.0 and precipitated protein was pelleted via centrifugation at 16000*g* for 10 min. The supernatant containing the [^{13}C]-prephenate was removed and purified as described above for unlabeled prephenate. 3 mL of prephenate containing fractions was frozen and lyophilized to dryness. The lyophilized prephenate and salt were resuspended in 300 μL of D_2O and placed in a 5 mm D_2O matched Shigemi tube for NMR analysis. ^1H and ^{13}C NMR data were referenced as described above.

Conversion of [^{13}C]-Prephenate to [^{13}C]-*ex*-H_2HPP and NMR Assignment. To produce [^{13}C]-*ex*-H_2HPP via nonenzymatic isomerization of [^{13}C]-*en*-H_2HPP, 2 mg of [^{13}C]-prephenate (purified as described above) was incubated with 10 μM BacA in 3 mL of 50 mM potassium phosphate buffer pH 8.0 for 24 h at 21 °C. The conversion of prephenate (no UV absorbance) to *en*-H_2HPP (λ_{max} = 258 nm) and then to *ex*-H_2HPP (λ_{max} = 295 nm) was monitored by UV absorbance.[14] The completed reaction was quenched and purified, and NMR data were acquired exactly as described above for prephenate, except UV absorbance at 295 nm (rather than LC/MS) was used to identify *ex*-H_2HPP elution in the purification.

Production and purification of [^{13}C]-*ex*-H_2HPP isomers 1 and 2 generated from enzymatic BacB isomerization of [^{13}C]-*en*-H_2HPP were performed as described above for the nonenzymatic isomerization reaction, except 5 mg of [^{13}C]-prephenate was used in a reaction volume of 5 mL and 10 μM BacB was added to the reaction. NMR data were acquired exactly as described above for prephenate.

Production, Purification, and NMR Assignments of Unlabeled *ex*-H_2HPP Isomers. The production and purification procedure described above for [^{13}C]-*ex*-H_2HPP isomers was repeated with unlabeled prephenate to obtain samples of unlabeled *ex*-H_2HPP isomers 1 and 2 for NMR data collection. Full NMR assignments were made using the same methods as described above for unlabeled chorismate and prephenate. Nuclear Overhauser effect (NOE) data reporting on the spatial distance between protons were obtained by acquiring a $^1H-^1H$-NOESY with a mixing time of 500 ms. Mass spectra of the isomers were obtained via LC/MS in negative ion detection mode using H_2O + 0.1% ammonium hydroxide as the mobile phase and acetonitrile + 0.1% ammonium hydroxide as the eluent.

Reactions comparing the production of *ex*-H_2HPP isomers 1 and 2 between BacA alone (with nonenzymatic diene isomerization) and BacAB in tandem were set up to contain 500 μM prephenate and 15 μM of each enzyme (incubated for 24 h at 21 °C). Reactions were quenched by addition of acetonitrile to 30% v/v, then frozen, and lyophilized to dryness. Dried mixtures were resuspended in 10 mM potassium phosphate buffer pH 8.0 and loaded onto a 100 × 2.1 mm analytical

Hypercarb column equilibrated in 10 mM potassium phosphate buffer pH 8.0. Compounds were eluted with a linearly increasing gradient of acetonitrile and elution monitored via UV absorbance at 295 nm. The 295 nm HPLC traces were integrated using the Karat 32 HPLC software from Beckman Coulter.

Kinetics of *ex*-H_2HPP Isomer Formation by BacAB. Kinetics of *ex*-H_2HPP isomer production from tandem BacAB incubation with prephenate were measured from a reaction containing 1 mM prephenate and 5 μM BacAB. The reaction was incubated at 21 °C, and reaction time points were taken by quenching 25 μL reaction aliquots with 50 μL of acetonitrile and vortexing. The quenched reactions were stored at −80 °C until all time points were quenched. Quenched aliquots were dried *in vacuo* and resuspended in 175 μL of 10 mM potassium phosphate buffer pH 8.0. The resuspended aliquots were analyzed by HPLC identically to the BacA vs BacAB reactions described in the previous paragraph.

Equilibration of 3*E*-7*R*- and 3*Z*-7*R*-*ex*-H_2HPP with BacB (and BacA). Production and purification of unlabeled *ex*-H_2HPP isomers were accomplished as described above for the production of [^{13}C]-*ex*-H_2HPP-isomers via tandem BacAB incubation, except 5 mg of unlabeled potassium prephenate was used as the starting material. The concentration of each *ex*-H_2HPP isomer was determined by UV absorbance ($\varepsilon_{295\ nm}$ = 15 300 M^{-1} cm^{-1} [14]). The reaction mixture for the equilibration time course consisted of 3 μM BacB (or BacA) in 50 mM potassium phosphate buffer pH 8.0. The reaction was initiated via addition of 400 μM *ex*-H_2HPP (either purified isomer 1 or 2). A control reaction was also setup containing no BacB to monitor non-enzymatic equilibration. Time points were taken by quenching 25 μL aliquots of the reaction with 50 μL of acetonitrile and vortexing. Quenched time points were stored at −80 °C until aliquots for all time points were collected. Samples were then dried *in vacuo* and resuspended in 75 μL of 10 mM potassium phosphate buffer pH 8.0. Resuspended samples were analyzed by HPLC exactly as described above for the BacA vs BacAB comparison reactions. The fraction of isomer 2 was calculated by dividing the integral value of the peak of isomer 2 by the sum of the integral values of the peaks of isomers 1 and 2 for each run. The data were fit to a first-order exponential decay equation using GraphPad Prism.

RESULTS AND DISCUSSION

Generation of [^{13}C]-Chorismates from [^{13}C]-Glucose Isotopomers. Our approach to determine which prochiral double bond in prephenate is isomerized during nonaromatizing decarboxylation by BacA was to use carbon magnetic resonance to distinguish between sp^3 and sp^2 carbon centers in the BacA product Δ^4,Δ^8-*en*-H_2HPP, since large shifts in the resonance positions were formerly seen in the ^{13}C NMR spectrum (for example, between C_6 (127.01 ppm) and C_8 (31.32 ppm)[14]). In turn, coupling of the BacA product to BacB action to generate the more stable Δ^3,Δ^5-*ex*-H_2HPP product would also allow the same carbon NMR approach. The acceleration of conversion of BacA-generated Δ^4,Δ^8-*endocyclic*-H_2HPP to the thermodynamically favored Δ^3,Δ^5-*exocyclic*-H_2HPP by BacB also prevents nonenzymatic breakdown of the *endo* isomer to phenylpyruvate and so provides quantitative flux to Δ^3,Δ^5-*ex*-H_2HPP.

For example, if one had a sample of 6-[^{13}C]-prephenate as substrate for BacA (and then tandem processing by BacB), isomerization of the pro-*R* double bond would yield an sp^3-labeled carbon in Δ^3,Δ^5-*ex*-H_2HPP while isomerization at the pro-*S* double bond (Figures 1B and 3) would instead yield the ^{13}C-enrichment at an sp^2 center, readily distinguishable by NMR spectroscopy. In case the BacA enzyme is not completely enantioselective, the ratio of [^{13}C] enrichment at the sp^3/sp^2 carbons in the BacB product would provide the degree of selectivity in the double-bond isomerization. Because the double bonds in the 1,4-diene ring system of prephenate are prochiral, a chemical synthesis to introduce [^{13}C] at one of the double bonds (but not the other) with absolute stereochemical control seemed daunting.

In contrast, the immediate metabolic precursor chorismate, convertible to prephenate by the 3,3-electrocyclic rearrangement catalyzed by chorismate mutase,[26] presented a more appealing target. While chemical synthesis of chorismate labeled at particular carbons with ^{13}C could be feasible,[27] we turned instead to a microbial biosynthetic route.

The biosynthetic path of glucose carbons into chorismate has been known for decades starting with the pioneering studies of Sprinson and colleagues;[28,29] randomization at the level of the C_3 triose phosphates during glycolysis gives doubling of label in shikimate and then tripling of label via the enolpyruvyl group found in chorismate even from singly labeled forms of glucose.[25] As a control to establish the methodology in our group, we fermented the readily available and relatively inexpensive 1-[^{13}C]-glucose with the classical *Aerobacter aerogenes* 62-1 blocked mutant strain[24] that accumulates chorismate in the medium. We saw enrichment at carbons 2, 6, and 9 in the NMR spectrum of chorismate as previously reported[25] (Figure S2), validating the approach. However, this labeling pattern would not solve the BacA regiochemistry question as it would go on to label C_5 and $C_{5'}$ of prephenate equally (and then carbons 3, 5, and 9 of Δ^3,Δ^5-*ex*-H_2HPP) (see Figure S4 for chorismate and prephenate numbering).

Instead, we reasoned that 5-[^{13}C]-glucose (a limiting reagent at the commercial price of $1950/g) would be a useful starting material to get to an appropriately labeled sample of prephenate by carrying out such fermentations. From 2 g of 5-[^{13}C]-glucose in a 250 mL fermentation, we obtained 56 mg of chorismate after purification on a preparative HPLC column. As anticipated, the chorismate sample had three ^{13}C atom enrichments of 57%, 70%, and 56% in the chorismate carbon NMR spectrum (Figures 3 and 4A), at carbons 1 (135.0 ppm), 5 (130.5 ppm), and 8 (153.9 ppm), respectively (see Figure S5A and Table S1 for full chorismate assignments). The carbon spectra were acquired with inverse-gated decoupling and a sufficiently long interscan delay time (150 s with no decoupler) to allow full carbon relaxation to achieve the full intensities of each of the carbon lines.[25] ^{13}C enrichment was calculated from a combination of the ^{13}C-linked proton satellite peaks of C_5 in the ^{1}H spectrum (Figure S4A) and signals from the inverse-gated decoupled carbon spectrum (Figure 4A).

Conversion of 1,5,8-[^{13}C]-Chorismate to 2,4,6-[^{13}C]-Prephenate. To convert this labeled [^{13}C]-chorismate sample to prephenate, we turned to chorismate mutase, which we cloned and overproduced from the *B. subtilis* bacilysin producer. Trial studies with unlabeled chorismate established that quantitative rearrangement of the chorismate scaffold to the prephenate scaffold occurred on a scale useful for carbon NMR, and the prephenate could be purified, isolated, and characterized (data not shown). Subsequent incubation of 2.1 mg of the 1,5,8 [^{13}C]-chorismate with 145 μg of pure chorismate mutase gave prephenate with the indicated carbon NMR resonances (Figure 4B). During the course of the 3,3-rearrangement, C_1 of chorismate becomes C_4 of prephenate,

dx.doi.org/10.1021/bi300254u | *Biochemistry* 2012, 51, 3241−3251

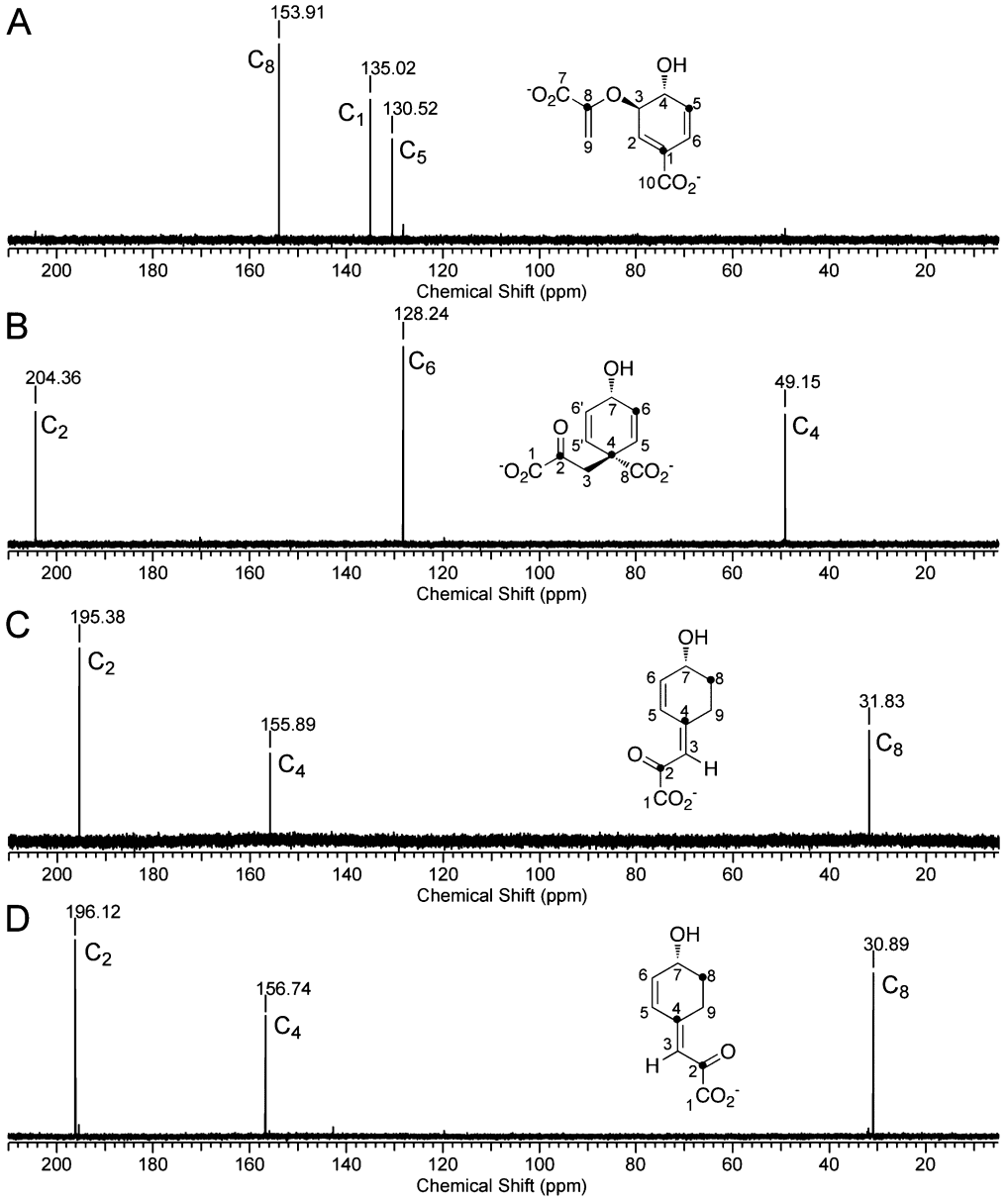

Figure 4. Inverse-gated decoupled carbon spectra of (A) 1,5,8-[^{13}C]-chorismate, (B) 2,4,6-[^{13}C]-prephenate, (C) 2,4,8-[^{13}C]-*ex*-H_2HPP isomer 1, and (D) 2,4,8-[^{13}C]-*ex*-H_2HPP isomer 2. 1,5,8-[^{13}C]-Chorismate was obtained from fermentation of 5-[^{13}C]-glucose with *A. aerogenes* 62−1; 2,4,6-[^{13}C]-prephenate from CM action on 1,5,8-[^{13}C]-chorismate; and 2,4,8-[^{13}C]-*ex*-H_2HPP isomers 1 and 2 from tandem BacAB action on 2,4,6-[^{13}C]-prephenate.

C_5 becomes C_6, and C_8 becomes the C_2 ketone. Figure 4B validates that the prephenate product has ^{13}C enrichment at carbons 2 (204.4 ppm), 6 (128.2 ppm), and 4 (49.2 ppm) (see Figure S5B and Table S2 for full prephenate NMR assignments).

Because of the symmetry of the cyclohexadiene ring of prephenate, carbons 6 and 6′ cannot be resolved in the NMR. Thus, without knowing the origin of this triply labeled ^{13}C-prephenate sample, one could not tell from the carbon NMR spectrum that only one of the two prochiral carbons, C_6 and $C_{6'}$, contained the ^{13}C enrichment. That differentiation can only be revealed by subsequent reactions that can distinguish the two prochiral olefins, (e.g., the nonaromatizing decarboxylase/isomerase BacA).

Processing of 2,4,6-[^{13}C]-Prephenate by BacA: Assignment of Product Stereochemistry at C_7 from Action of BacA. Tandem incubation of the triply labeled [^{13}C]-prephenate with purified *B. subtilis* enzyme BacA followed by nonenzymatic isomerization allowed HPLC purification of Δ^3,Δ^5-*ex*-H_2HPP. The carbon NMR spectrum (Figure S3A) of this compound, which turns out to be the 3*E*-olefinic isomer as detailed in the following paragraphs, shows three peaks, at 30.9 (C_8), 156.8 (C_4), and 196.1 (C_2) ppm vs a CH_3CN standard. By comparison with our assignment of the carbon NMR spectrum of unlabeled material (Figure S5D and Table S4), these resonances correspond to carbons 2, 4, and 8 of Δ^3,Δ^5-*ex*-H_2HPP. The diagnostic resonance is the ^{13}C enrichment at the sp^3 carbon 8 of *ex*-H_2HPP. There is no detectable enrichment at the sp^2 C_6.

Therefore, it is clear that BacA is an enantioselective decarboxylation and isomerization catalyst. As decarboxylation proceeds, the electrons released in the C_4−COO bond cleavage move into the ring, creating the new double bond, and the electrons in the original pro-*R* double bond are used to pick up a proton (path 1 of Figure 1B) at C_6 of prephenate. From the

dx.doi.org/10.1021/bi300254u | *Biochemistry* 2012, 51, 3241−3251

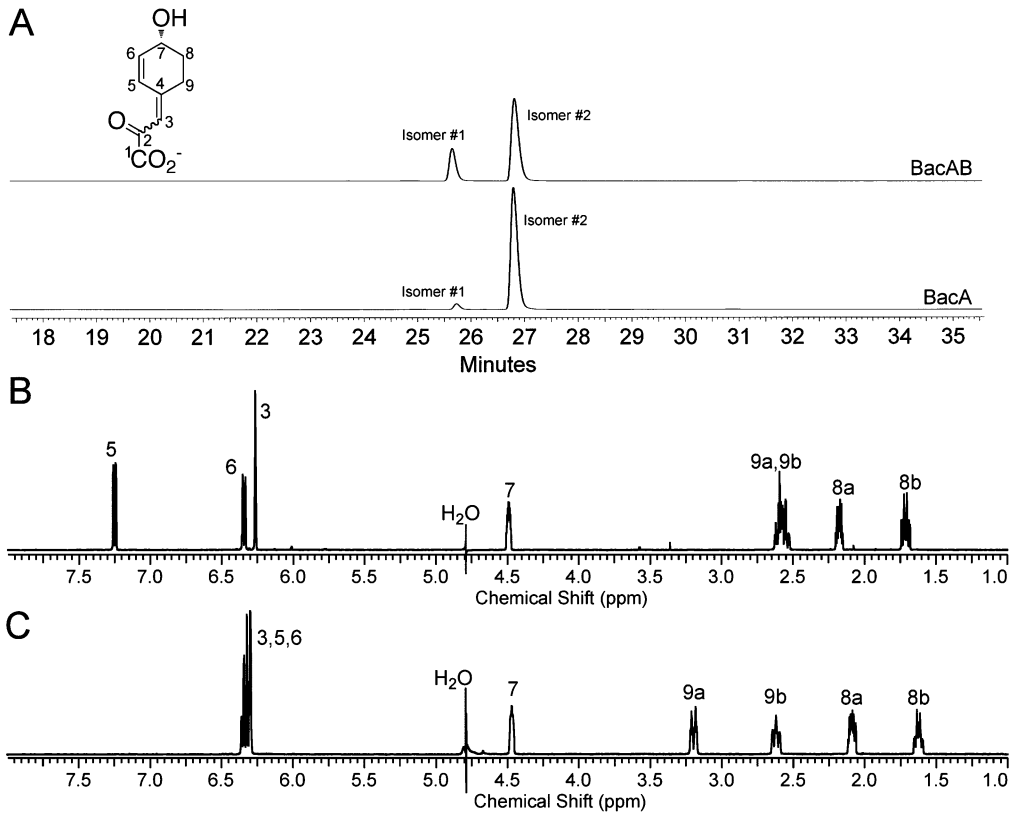

Figure 5. (A) HPLC separation (295 nm UV trace) of *ex*-H_2HPP isomers 1 and 2 produced via action of BacA alone (5%/95% of isomers 1/2) or tandem BacAB action (26%/74% of isomers 1/2) on prephenate after 24 h incubation at 21 °C. (B) ^{1}H NMR of unlabeled *ex*-H_2HPP isomer 1. (C) ^{1}H NMR of unlabeled *ex*-H_2HPP isomer 2. *ex*-H_2HPP isomers in (B) and (C) were produced by the tandem action of BacAB on prephenate.

perspective of C_7 this is the *R*-isomer. No 7*S*-OH product appears to be generated.

Detection and NMR Assignment of Geometric Isomers of Δ^3,Δ^5-H_2HPP from Action of BacB. When BacB was added to the BacA incubations with the 2,4,6-[^{13}C]-prephenate to accelerate the allylic isomerization of the *en*-H_2HPP to the more stable *ex*-H_2HPP product, in contrast to the single product peak detected with BacA and nonenzymatic isomerization, the BacAB tandem incubation gave rise to two peaks separable by HPLC as shown in Figure 5A. Because of the substantial polarity of the H_2HPP isomers, a Hypercarb column proved to be the support on which isomer separation could be achieved. These are labeled as isomer 1 and isomer 2 because they have the same molecular mass (observed *m*/*z* 181.0503; calculated *m*/*z* 181.0506) by LC/MS analysis. Also as seen in Figures 4C and 4D they have comparable carbon NMR spectra, indicating the pro-*R* double bond has moved (BacA action as expected) and both isomers are 7*R*-alcohol forms of *ex*-H_2HPP.

It seemed likely that isomer 1 and 2 might be the 3*E*/3*Z* geometric isomers around the exocyclic double bond in *ex*-H_2HPP. The first indication confirming this was the proton NMR spectra (Figures 5B,C). Isomer 1 and isomer 2 have equivalent resonances for alcoholic H7 and the methylene hydrogens 8a and 8b. The dispersion for protons 3, 5, and 6 are radically different and the splitting pattern for the methylene hydrogens 9a and 9b are also distinct, consistent with different geometries at the 3,4-olefin. NOESY spectra are shown in Figure 6A for isomer 1 and Figure 6B for isomer 2. Most diagnostic is the NOE cross-peak between the olefinic H3 and one of the H9 resonances (indistinguishable due to identical chemical shifts) for isomer 1 that is absent in isomer 2. Thus, isomer 1 is assigned as the 3*Z*-7*R* diastereomer and isomer 2 the 3*E*-7*R* diastereomer of *ex*-H_2HPP. (Complete NMR spectral data for isomer 1 are presented in Figure S5C and Table S3.)

Although both 3*Z*- and 3*E*-*ex*-H_2HPP isomers are present after long incubations containing BacA and BacB, kinetic analysis (Figure 7A) indicates that the 3*E* isomer is formed first (at about a 50/1 *E*/*Z* ratio) and the 3*Z*-geometric isomer grows in slowly. The initial product was confirmed as *ex*-H_2HPP (λ_{max} = 295 nm) and not *en*-H_2HPP (λ_{max} = 258 nm) by UV absorption[14] (data not shown). The 3*Z* isomer then grows in over a period of ∼17 h under the particular experimental conditions. Comparing the 17 and 40 h time points suggest an equilibrium has been approached with a ratio of ∼3/1 of the *E*/*Z*-isomers of *ex*-H_2HPP.

BacB-Mediated Equilibration of 3*E*-7*R*- and 3*Z*-7*R*-*ex*-H_2HPP. From the trace in Figure 7A, it appeared that BacB could in fact catalyze equilibration between the initially formed 3*E* and the late-appearing 3*Z* isomers. As shown in Figure 7B starting from 85% pure *Z*-isomer, BacB alone catalyzed the conversion of *Z*- to *E*-isomer until equilibrium was reached. (4% nonenzymatic conversion of the *Z*-isomer was observed as background during the 24 h interval.) Going in the opposite direction, when BacB was added to 85% pure *E*-isomer it was converted to the *Z*-isomer until equilibrium was reached (Figure 7C). (0.1% nonenzymatic conversion of the *E*-isomer was observed as background during the 24 h interval.) For the incubation of BacB with both the *Z*- (isomer 1) and *E*-isomer (isomer 2) of *ex*-H_2HPP, equilibrium was obtained at the same 3/1 ratio of *E*/*Z* geometric isomers (Figure 7D) as was observed for the reaction from prephenate with BacAB (Figure 7A).

dx.doi.org/10.1021/bi300254u | *Biochemistry* 2012, 51, 3241−3251

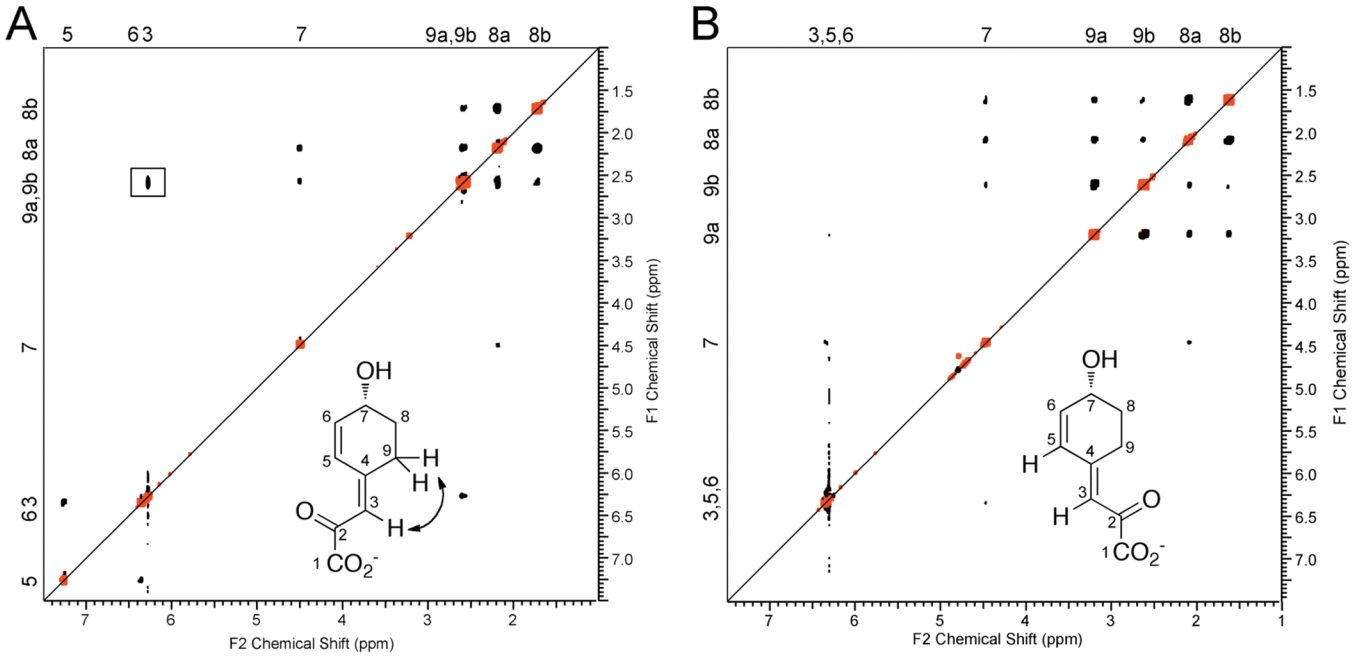

Figure 6. $^{1}H-^{1}H$-NOESY spectra of *ex*-H_2HPP isomer 1 (A) and isomer 2 (B) produced from the tandem action of BacAB on prephenate. (A) NOE interaction between protons 3 and 9 of isomer 1 (cross-peak is boxed) identify the Δ^3-olefin as possessing "*Z*" geometry. (B) NOE interaction between protons 3 and 5 could not be distinguished due to overlapping resonances. However, a NOE cross-peak between protons 3 and 9 is absent, indicating "*E*" geometry for the Δ^3-olefin.

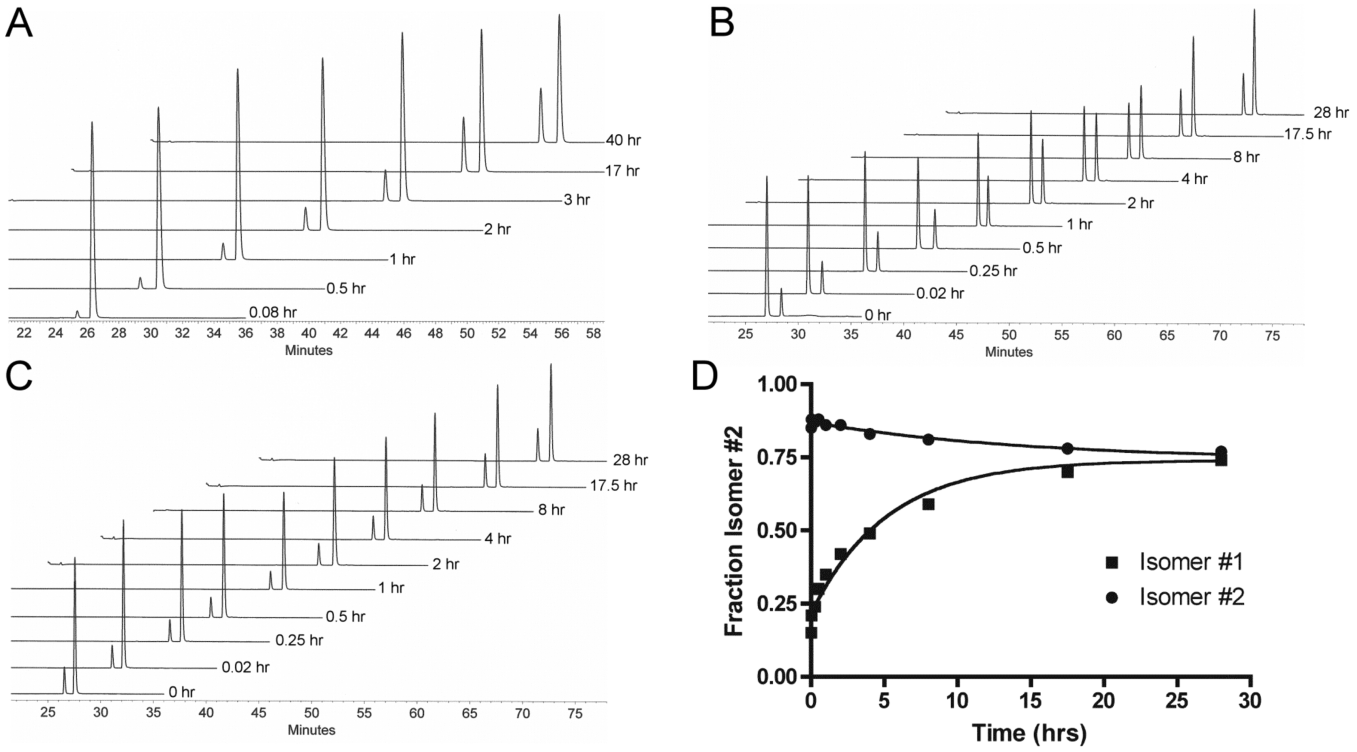

Figure 7. (A) HPLC traces (295 nm) showing the kinetics of *ex*-H_2HPP isomer 1 and 2 formation from the tandem action of 5 μM BacAB on 1 mM prephenate at 21 °C. (B) HPLC traces (295 nm) showing the equilibration of 400 μM *ex*-H_2HPP isomer 1 with 3 μM BacB at 21 °C. (C) HPLC traces (295 nm) showing the equilibration of 400 μM *ex*-H_2HPP isomer 2 with 3 μM BacB at 21 °C. (D) Kinetics of equilibration of *ex*-H_2HPP isomers 1 and 2 with BacB. Data were fit to a first-order exponential decay equation yielding $t_{1/2}$ values of 3.6 and 10.4 h for the equilibration of isomers 1 and 2, respectively.

Pure BacA has no ability to interconvert the 3*E* and 3*Z*-*ex*-H_2HPP isomers (data not shown).

A possible route from the 3*E*-*ex*-H_2HPP initial product to the 3*Z*-olefin regioisomer is shown in Figure 8. BacB must be able

dx.doi.org/10.1021/bi300254u | *Biochemistry* 2012, 51, 3241−3251

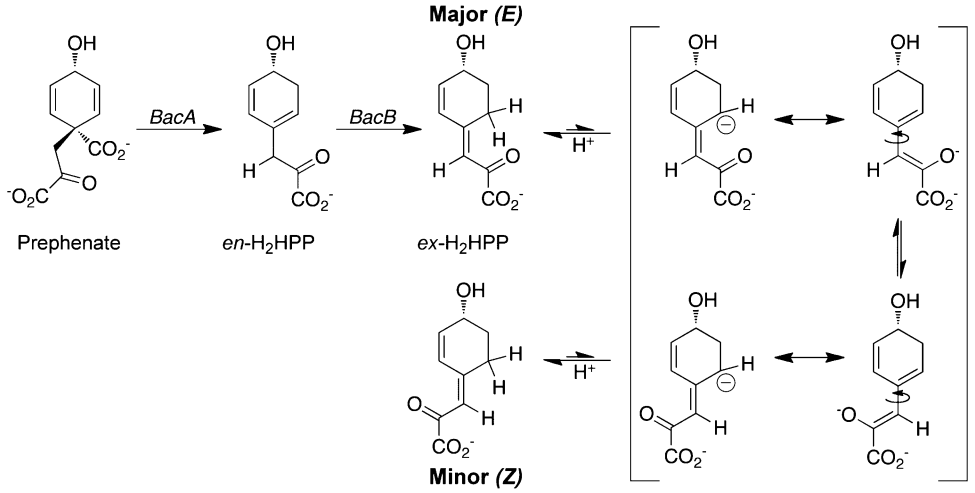

Figure 8. Tandem action of BacAB with prephenate initially yields only the *E*-isomer of *ex*-H_2HPP. BacB is then able to equilibrate between the *E*- and *Z*-isomers of *ex*-H_2HPP via a proposed dienolate intermediate generated by abstraction of a proton from C_9.

to act on the 3*E* product isomer by abstraction of one of the acidic C_9 methylene hydrogens as a proton to yield the C_9 carbanion, which has the indicated dienolate as a resonance contributor. The dienolate can rotate around the C_3-C_4 single bond to give a mixture of *E*- and *Z*-dienolates. Protonation at C_9 would yield either the 3*E*- or 3*Z*-*ex*-H_2HPP conjugated products, depending on dienolate composition. At 3 μM [BacB] and 400 μM [*ex*-H_2HPP], the half-time for equilibration was found to be 3.6 h in the *Z*- to *E*-direction. The 133/1 ratio of substrate to enzyme suggests about 0.3 equilibration events per minute under the given conditions.

From BacA incubations in the absence of BacB and at initial time points with BacB the 3*E*-/3*Z*-isomer ratio is about 50/1, indicating a kinetically favored path to 3*E*. The question arises why BacB is retained in the biosynthetic pathway, accelerating the flux by 10^3 to the 3*E*-*ex*-H_2HPP regioisomer. It may be that the subsequent equilibration of up to 25% of the 3*Z*-7*R*-*ex*-H_2HPP product by BacB suggests that one or more of the downstream enzymes in the bacilysin (or related biosynthetic pathways) pathway may care about the *E*/*Z* olefin geometry. That is the subject of future efforts now that the isomers have been detected, structures assigned, and kinetics of equilibration determined.

CONCLUSIONS

This study establishes that BacA is indeed an enantioselective pro-*R* olefin isomerase during prephenate nonaromatizing decarboxylation. It is likely that the selective isomerization of the pro-*R* olefin in prephenate by BacA reflects an active site orientation where the enzyme−substrate complex with bound prephenate brings a side chain conjugate acid (BH^+) adjacent to C_6 of prephenate in the active site. Determination of the 7*R*-stereochemistry in Δ^3,Δ^5-*ex*-H_2HPP, and by extension its predecessor Δ^4,Δ^8-*en*-H_2HPP with no detectable 7*S*-isomer, indicates a high degree of olefin selectivity. This occurs as BacA concomitantly and surprisingly suppresses the aromatization fate that is characteristic of canonical prephenate decarboxylases in biosynthetic pathways to phenylalanine.

BacB, the next enzyme in the bacilysin biosynthetic pathway, takes the Δ^4,Δ^8- *endocyclic*-H_2HPP and first generates the 3*E*-geometric isomer. BacB will then catalyze the formation of the 3*Z*- from the 3*E*-olefin and proceed to equilibrate between the 3*E* and 3*Z* isomers around the 3,4-exocyclic double bond. We anticipate this reflects the reversible ability to generate the dienolate intermediates in the BacB active site and reprotonate at C_9. BacB speeds up the 1,3-allylic isomerization some 10^3 over the nonenzymatic rate, which otherwise yields the *E*-olefin at about a 50/1 kinetic ratio over the *Z*-isomer, far away from the 3/1 thermodynamic ratio.

These findings on BacA and BacB set the stage for evaluation of subsequent issues of stereochemistry and mechanism in these nonaromatizing pathways arising from decarboxylation of prephenate to anticapsin/bacilysin and other dihydroaromatic amino acids. As prephenate is processed by BacA and BacB, the $C_5H{=}C_6H$ (pro-*R*) olefin gets saturated to a CH_2-CH_2 pair of carbon atoms. Protonation occurs first at C_8 of *en*-H_2HPP and then at C_9 as *ex*-H_2HPP is formed. Because both C_8 and C_9 are methylene groups in the BacB product, in tetrahydrotyrosine, and then in anticapsin, the stereochemistry is cryptic when incubations are conducted in H_2O. In D_2O it should next be possible to determine chirality and thus orientation of the active site BD^+ groups relative to the plane of the cyclohexadiene ring of bound substrates in BacA and BacB, respectively, as constraints on mechanism and comparisons to how canonical prephenate aromatizing decarboxylases work.

The mix of *E*- and *Z*-geometries in the Δ^3,Δ^5-*ex*-H_2HPP generated by BacB is also cryptic in the overall pathway since that olefin gets reduced in the next step by delivery of a hydride ion from NADH to C_4. However, that *E*- vs *Z*-olefin geometry could influence the stereochemistry at C_4 in the reductive step catalyzed by YwfH (Figure 1A), and evaluation of that outcome will also be a subject of future efforts. Currently, only natural products with tetrahydrotyrosine of the 4*S*-configuration have been assigned.[20,30] However, other natural products containing tetrahydrotyrosine with unassigned stereochemistry at C_4 are known,[31,32] and how stereochemistry is controlled at that center during biosynthesis is a mystery.

Ultimately stereochemical and mechanistic studies need to be coupled with BacA structural studies to give insights into how electrons released into the cyclohexadiene ring on decarboxylation of prephenate are diverted out of the canonical aromatization manifold and quenched instead by regioselective protonation at C_6 in this newly appreciated enzyme subfamily.

dx.doi.org/10.1021/bi300254u | *Biochemistry* 2012, 51, 3241−3251

■ ASSOCIATED CONTENT

Supporting Information

SDS-PAGE analysis of chorismate mutase purification; additional ^{13}C and ^{1}H NMR spectra of ^{13}C labeled and unlabeled chorismate, prephenate, 3*Z*-7*R*-*ex*-H_2HPP, and 3*E*-7*R*-*ex*-H_2HPP; and tabulated NMR spectral data for unlabeled chorismate, prephenate, 3*Z*-7*R*-*ex*-H_2HPP, and 3*E*-7*R*-*ex*-H_2HPP. This material is available free of charge via the Internet at http://pubs.acs.org.

■ AUTHOR INFORMATION

Corresponding Author

*E-mail: Christopher_Walsh@hms.harvard.edu; Ph: 617.432.1715; Fax: 617.432.0483.

Funding

This work was supported in part by National Institutes of Health Grants AI042738 and GM49338 (C.T.W.).

Notes

The authors declare no competing financial interest.

■ ACKNOWLEDGMENTS

We thank Drs. Sarah A. Mahlstedt, Stuart W. Haynes, Timothy A. Wencewicz, and Steven J. Malcolmson for helpful advice and discussions. We again thank TAW and SJM for careful reading of the manuscript.

■ ABBREVIATIONS

B. subtilis, *Bacillus subtilis*; *E. coli*, *Escherichia coli*; *A. aerogenes*, *Aerobacter aerogenes*; H_2HPP, dihydro-4-hydroxyphenylpyruvate; H_4HPP, tetrahydro-4-hydroxyphenylpyruvate; H_4Tyr, tetrahydrotyrosine; IPTG, isopropyl-β-D-galactopyranoside; SDS-PAGE, sodium dodecyl sulfate−polyacrylamide gel electrophoresis; LC/MS, liquid chromatography/mass spectrometry; NMR, nuclear magnetic resonance; gCOSY, gradient homonuclear correlation spectroscopy; gHSQC, gradient heteronuclear single-quantum coherence; gHMBC, gradient heteronuclear multiple bond coherence; NOESY, nuclear Overhauser effect spectroscopy; FPLC, fast protein liquid chromatography; HPLC, high performance liquid chromatography; PCR, polymerase chain reaction; NADH, reduced nicotinamide adenine dinucleotide; CM, chorismate mutase; D_2O, deuterium oxide.

■ REFERENCES

(1) Walker, J., and Abraham, E. (1970) Isolation of Bacilysin and a New Amino Acid from Culture Filtrates of Bacillus-Subtilis. *Biochem. J. 118*, 557−561.

(2) Hilton, M., Alaeddinoglu, N., and Demain, A. (1988) Synthesis of Bacilysin by Bacillus-Subtilis Branches from Prephenate of the Aromatic Amino-Acid Pathway. *J. Bacteriol. 170*, 482−484.

(3) Roscoe, J., and Abraham, E. (1966) Experiments Relating to Biosynthesis of Bacilysin. *Biochem. J. 99*, 793−800.

(4) Chmara, H., Woynarowska, B., and Borowski, E. (1981) Epoxypeptide Antibiotic Tetaine Mimics Peptides in Transport to Bacteria. *J. Antibiot. 34*, 1608−1612.

(5) Perry, D., and Abraham, E. (1979) Transport and Metabolism of Bacilysin and Other Peptides by Suspensions of Staphylococcus-Aureus. *J. Gen. Microbiol. 115*, 213−221.

(6) Chmara, H., Smulkowski, M., and Borowski, E. (1980) Growth Inhibitory Effects of Amidotransferase Inhibition in Candida-Albicans by Epoxypeptides. *Drugs Exp. Clin. Res. 6*, 7−14.

(7) Kenig, M., Vandamme, E., and Abraham, E. (1976) Mode of Action of Bacilysin and Anticapsin and Biochemical Properties of Bacilysin-Resistant Mutants. *J. Gen. Microbiol. 94*, 46−54.

(8) Chmara, H. (1985) Inhibition of Glucosamine Synthase by Bacilysin and Anticapsin. *J. Gen. Microbiol. 131*, 265−271.

(9) Chmara, H., Zahner, H., and Borowski, E. (1984) Anticapsin, an Active-Site Directed Irreversible Inhibitor of Glucosamine-6-Phosphate Synthetase from Escherichia-Coli. *J. Antibiot. 37*, 1038−1043.

(10) Edwards, J., and Jackman, L. (1965) Chorismic Acid. A Branch Point Intermediate in Aromatic Biosynthesis. *Aust. J. Chem. 18*, 1227−1239.

(11) Gibson, M., and Gibson, F. (1964) Preliminary Studies on Isolation and Metabolism of Intermidiate in Aromatic Biosynthesis - Chorismic Acid. *Biochem. J. 90*, 248−256.

(12) Knaggs, A. (2001) The Biosynthesis of Shikimate Metabolites. *Nat. Prod. Rep. 18*, 334−355.

(13) Steinborn, G., Hajirezaei, M., and Hofemeister, J. (2005) Bac Genes for Recombinant Bacilysin and Anticapsin Production in Bacillus Host Strains. *Arch. Microbiol. 183*, 71−79.

(14) Mahlstedt, S. A., and Walsh, C. T. (2010) Investigation of Anticapsin Biosynthesis Reveals a Four-Enzyme Pathway to Tetrahydrotyrosine in Bacillus Subtilis. *Biochemistry. 49*, 912−923.

(15) Mahlstedt, S., Fielding, E. N., Moore, B. S., and Walsh, C. T. (2010) Prephenate Decarboxylases: A New Prephenate-Utilizing Enzyme Family that Performs Nonaromatizing Decarboxylation En Route to Diverse Secondary Metabolites. *Biochemistry. 49*, 9021−9023.

(16) Crawford, J. M., Mahlstedt, S. A., Malcolmson, S. J., Clardy, J., and Walsh, C. T. (2011) Dihydrophenylalanine: A Prephenate-Derived Photorhabdus Luminescens Antibiotic and Intermediate in Dihydrostilbene Biosynthesis. *Chem. Biol. 18*, 1102−1112.

(17) Van Vleet, J., Kleeb, A., Kast, P., Hilvert, D., and Cleland, W. W. (2010) (13)C Isotope Effect on the Reaction Catalyzed by Prephenate Dehydratase. *Biochim. Biophys. Acta, Proteins Proteomics 1804*, 752−754.

(18) Hermes, J., Tipton, P., Fisher, M., Oleary, M., Morrison, J., and Cleland, W. (1984) Mechanisms of Enzymatic and Acid-Catalyzed Decarboxylations of Prephenate. *Biochemistry 23*, 6263−6275.

(19) Rajavel, M., Mitra, A., and Gopal, B. (2009) Role of Bacillus Subtilis BacB in the Synthesis of Bacilysin. *J. Biol. Chem. 284*, 31882−31892.

(20) Ishida, K., Christiansen, G., Yoshida, W. Y., Kurmayer, R., Welker, M., Valls, N., Bonjoch, J., Hertweck, C., Boerner, T., Hemscheidt, T., and Dittmann, E. (2007) Biosynthesis and Structure of Aeruginoside 126A and 126B, Cyanobacterial Peptide Glycosides Bearing a 2-Carboxy-6-Hydroxyoctahydroindole Moiety RID E-9795−2011. *Chem. Biol. 14*, 565−576.

(21) Gray, J., Golinellipimpaneau, B., and Knowles, J. (1990) Monofunctional Chorismate Mutase from Bacillus-Subtilis - Purification of the Protein, Molecular-Cloning of the Gene, and Overexpression of the Gene-Product in Escherichia-Coli. *Biochemistry 29*, 376−383.

(22) Gottlieb, H., Kotlyar, V., and Nudelman, A. (1997) NMR Chemical Shifts of Common Laboratory Solvents as Trace Impurities. *J. Org. Chem. 62*, 7512−7515.

(23) Liu, J., Quinn, N., Berchtold, G., and Walsh, C. (1990) Overexpression, Purification, and Characterization of Isochorismate Synthase (Entc), the 1st Enzyme Involved in the Biosynthesis of Enterobactin from Chorismate. *Biochemistry 29*, 1417−1425.

(24) Gibson, F. (1964) Chorismic Acid - Purification + some Chemical + Physical Studies. *Biochem. J. 90*, 256−261.

(25) Rajagopalan, J., and Jaffe, E. (1993) Microbial-Production and Nmr Characterization of [2,6,9-C-13]Chorismate and [1,3,5,8-C-13]-Chorismate. *Bioorg. Med. Chem. Lett. 3*, 1453−1456.

(26) Lee, A., Stewart, J. D., Clardy, J., and Ganem, B. (1995) New Insight into the Catalytic Mechanism of Chorismate Mutases from Structural Studies. *Chem. Biol. 2*, 195−203.

(27) Gustin, D., and Hilvert, D. (1999) Chemoenzymatic Synthesis of Isotopically Labeled Chorismic Acids. *J. Org. Chem. 64*, 4935−4938.

(28) Srinivasan, P., Shigeura, H., Sprecher, M., Sprinson, D., and Davis, B. (1956) Biosynthesis of Shikimic Acid from D-Glucose. *J. Biol. Chem. 220*, 477−497.

(29) Herrmann, K. (1995) The Shikimate Pathway - Early Steps in the Biosynthesis of Aromatic-Compounds. *Plant Cell. 7*, 907−919.
(30) Baldwin, J., Adlington, R., and Mitchell, M. (1993) Stereocontrolled Enantiospecific Synthesis of Anticapsin - Revision of the Configuration. *J. Chem. Soc., Chem. Commun.*, 1332−1335.
(31) Namikoshi, M., Sun, F., Choi, B., Rinehart, K., Carmichael, W., Evans, W., and Beasley, V. (1995) 7 More Microcystins from Homer-Lake Cells - Application of the General-Method for Structure Assignment of Peptides Containing Alpha,Beta-Dehydroamino Acid Unit(s). *J. Org. Chem. 60*, 3671−3679.
(32) Harada, K., Mayumi, T., Shimada, T., Suzuki, M., Kondo, F., and Watanabe, M. (1993) Occurrence of 4 Depsipeptides, Aeruginopeptins, Together with Microcystins from Toxic Cyanobacteria. *Tetrahedron Lett. 34*, 6091−6094.